

## Local angle domain imaging and fracture prediction in Tarim Basin

Wensheng Duan\* and Genxin Peng, Tarim Oilfield Company, Petrochina; Xiaoping Song and Xueqiang Li, Paradigm Technology, Beijing

### Summary

The horizontal transverse isotropy (HTI) feature of seismic data are notable in carbonate fracture reservoirs, and diffractions in pre-stack seismic data make carbonate carve reservoirs much different from horizontal reflectors. Based on these seismic features, local angle domain imaging introduce a new approach for high resolution interpretation and delineation for carbonate fracture and carve reservoir's research. The output of local angle domain imaging are full-azimuth opening angle and dip angle gathers. Opening angle gathers can be used for velocity tomography inversion and AVAZ inversion. Dip angle gathers are used to separate specular and diffraction energy, which will be useful for specular enhancement and diffraction imaging.

### Introduction

In YM area of Tarim basin, the Ordovician carbonate formations are controlled by strike-slip faults and their concomitant faults. Water eroded horizontally along faults in early stage and carves grew, later hydrocarbon moved upwards along faults and reservoirs took shape. According to the previous study, the main focus and challenge for geophysicists and geologists is how to delineate fractures and carves in this area.

In ray theory, incidence and outgoing rays are symmetrical, which is specular reflection. When geologic body has a similar size of wave length, outgoing rays will propagate in all directions, which is diffraction. Specular reflection and diffraction can be indicated easily in local dip angle domain. The output of local angle domain imaging are full-azimuth opening angle and dip angle gathers. Analysis and AVAZ inversion based on opening angle gathers (reflection gathers) are used for azimuthal anisotropy analysis and fracture orientation and density research. Stacking at different dip levels based on dip angle gathers may reveal additional information of the subsurface by unmasking different source of energy, and avoid loss of useful information from the full wavefield of depth migrated data. Interpreter could derive to a much accurate interpretation and precise delineation of the subsurface structure.

For real data in YM area, we take advantage of local angle domain imaging to separate reflections and diffractions energy, and delineate the distribution of carbonate caves. Fracture prediction is also conducted, which successfully reveals the details of fracture and coincides with FMI data. Therefore we can plan wells with more confidence.

### Local Angle Domain Imaging

Typical CIP gathers generated by Kirchhoff PSDM is 4D data, that is  $x, y, z$  and offset. For Kirchhoff PSDM in OVT domain, these gathers will be 5D data. The additional dimension is azimuth, thanks to the azimuth-keeping feature of OVT<sup>[1]</sup> imaging. But in local angle domain, imaging space is 7D, including  $x, y, z, \gamma_1, \gamma_2, v_1$  and  $v_2$ , where  $x, y, z$  mark reflector position,  $\gamma_1, \gamma_2$  represent opening angle and opening azimuth of ray pair,  $v_1, v_2$  the dip angle and azimuth<sup>[2]</sup>, as shown in Figure 1.

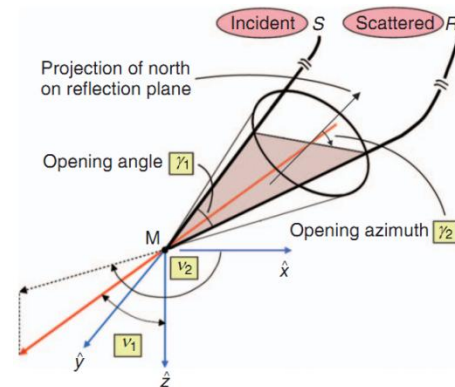


Figure 1: Local angle domain with 7 dimension

It is no doubt that 7D imaging requires huge storage capability and intensive computation resource, and almost impossible for practical processing. Therefore we use double integration to reduce the number of dimension. We will obtain opening angle gathers when we integrate  $\gamma_1$  and  $\gamma_2$ , and dip angle gathers when integrating  $v_1, v_2$ . Opening angle gathers or reflection gathers are used for velocity tomography inversion and AVAZ inversion, and dip angle gathers provide potentials to separate specular and diffraction energy.

In order to be able to discriminate between the different wave fields along the dip angle gathers, first let's recognize how those are manifested. Think of three reflectors with high dip angle, small dip angle and zero degree dip angle, their reflections in dip angle gathers will have specular features: reflection energy spread as a curve, and the lowest point of the curve has the same dip angle as interface's dip angle. (Figure 2).

## Local angle domain imaging and fracture prediction in Tarim Basin

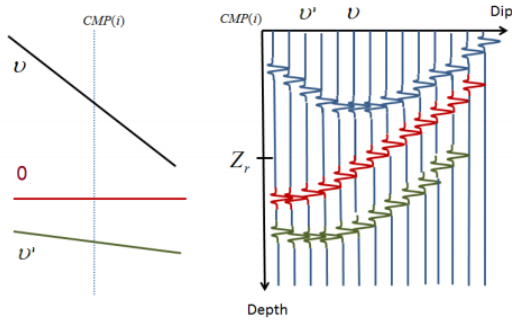


Figure 2: Wave field of specular reflection in dip angle gathers

But when seismic wave encounters small discontinuities with similar size of wave length, such as faults, wedge-out boundary, Karst carves, diffraction will occur. Diffraction energy spreads equally at all dips and azimuths (Figure 3).

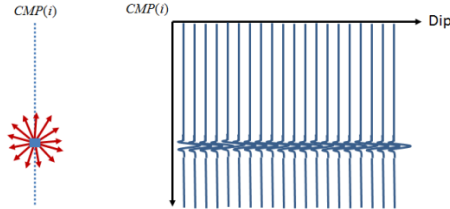


Figure 3: Wave field of diffraction in dip angle gathers

Now that we can recognize the characteristics of the different energy fields, we could stack and discriminate the wave field accordingly. By applying high dip mutes, we can obtain specular weighted enhancement, and by applying low dip mutes, we can get fault systems with enhancements of discontinuity and Karst with high resolution images.

For real data in YM area, Karst carves are developed abundantly in carbonate formations, its diffraction feature is outstanding in full-azimuth dip angle domain.

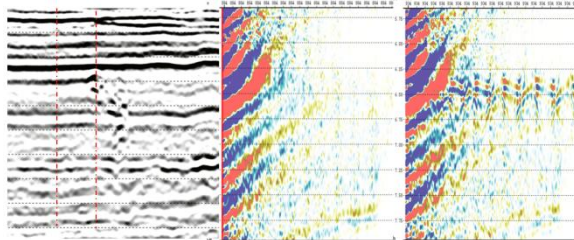


Figure 4: Dip angle gathers without (middle) and with cave scatters (right), their position shown in the section (left)

Specular reflection layers are generally horizontal in this survey, so its bottom is at minimum dip angle and the gather shows half of a curve. When cave exists, diffraction occurs and spreads equally at all directions. Diffraction can be easily distinguished from specular reflection. Specular

reflection energy is so strong when everything is stacked that Karst caves which exhibit small energy do look blurred, on the other hand when stacking high dips, reflections are almost eliminated, Karst energy is stronger than apparent dip reflections and noise. So an image of diffraction without specular reflection is achievable. Because of small dip angle of reflection layers, partial dip stack is a reasonable way for diffraction enhancement. A  $14^\circ - 45^\circ$  partial dip stack highlights Karst carves very well. From figure 5, we can see that the strong reflection mask over the caves, make it look not-clear-enough where the reflections are very strong. Once they are removed, there is nothing which interfere with the cave's energy, and it looks much more outstanding in the circle.

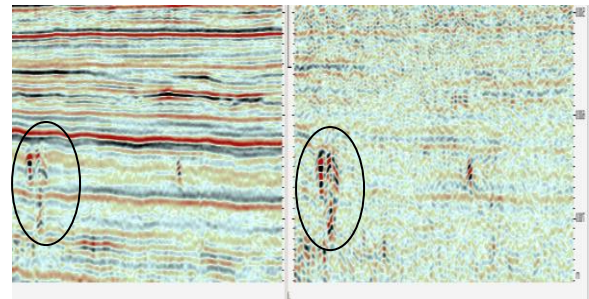


Figure 5: Full-wavefield stack vs partial-dip ( $14^\circ - 45^\circ$ ) stack

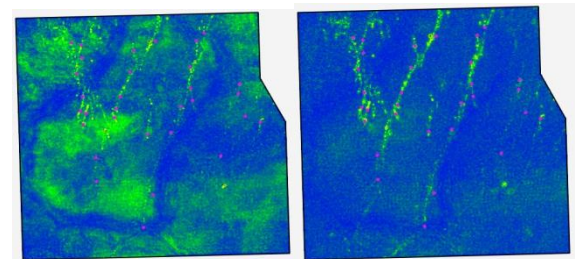


Figure 6: RMS-amplitude slice of full-wavefield stack vs partial-dip stack

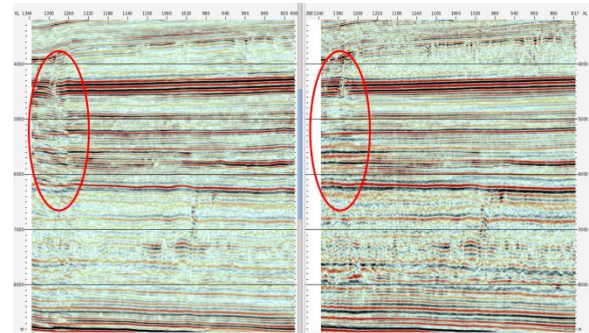


Figure 7: Comparison of KPSDM and local angle domain PSDM

## Local angle domain imaging and fracture prediction in Tarim Basin

From comparison of RMS-amplitude slice of full-wavefield stack and partial-dip stack in figure 6, it is clearly visible that the strong reflection of full wavefield stack mask over the Karst, make it looks discontinuous. Once they are removed, and it looks continuous and much more focused.

Figure 7 compares Kirchhoff PSDM and local angle domain PSDM. The false fault in the circle existed in KPSDM section is eliminated in local angle domain PSDM one, and event continuity is also improved.

### HTI Model and AVAZ Inversion

A formation with vertical fractures is defined as HTI media. The P wave reflection responding<sup>[3]</sup> is

$$R_p(\theta, \phi) = \frac{1}{2} \frac{\Delta(\rho\alpha)}{\rho\alpha} + \frac{1}{2} \left\{ \frac{\Delta\alpha}{\alpha} - \left( \frac{2\beta}{\alpha} \right)^2 \frac{\Delta(\rho\beta^2)}{\rho\beta^2} + \left[ \Delta\delta^{(v)} + 2 \left( \frac{2\beta}{\alpha} \right)^2 \cdot \Delta\gamma \right] \cos^2 \phi \right\} \sin^2 \theta + \frac{1}{2} \left\{ \frac{\Delta\alpha}{\alpha} + \Delta\varepsilon^{(v)} \cos^4 \phi + \Delta\delta^{(v)} \sin^2 \phi \cos^2 \phi \right\} \sin^2(\theta) g^2(\theta) \quad (1)$$

This equation 1 is a third order normal incident long offset linear approximation equation. Where  $\theta$  is incident angle,  $\phi$  is angle between incident azimuth and symmetry axis. While incident is parallel to symmetry axis  $\phi=0^\circ$ , the equation becomes

$$R_p(\theta, 0) = \frac{1}{2} \frac{\Delta(\rho\alpha)}{\rho\alpha} + \frac{1}{2} \left\{ \frac{\Delta\alpha}{\alpha} - \left( \frac{2\beta}{\alpha} \right)^2 \left( \frac{\Delta(\rho\beta^2)}{\rho\beta^2} - 2\Delta\gamma \right) + \Delta\delta^{(v)} \right\} \sin^2 \theta + \frac{1}{2} \left\{ \frac{\Delta\alpha}{\alpha} + \Delta\varepsilon^{(v)} \right\} \sin^2(\theta) g^2(\theta) \quad (2)$$

In this case, amplitude variation with angle (AVA) depends on  $\delta$ ,  $\varepsilon$  and  $\gamma$ . Where  $\delta$ ,  $\gamma$  describe AVA gradient,  $\varepsilon$  is a part of third term. The third term could be discarded, and the equation becomes

$$R(\theta, \phi) = NI + B(\phi) \sin^2 \theta \quad (3)$$

Where  $B(\phi) = B^{iso} + B^{ani} \cos^2(\phi)$ ,

Set  $B_1 = B$ ,  $B_2 = B^{ani} + B$ ,  $B(\phi)$  is written as

$$B(\phi) = B_1 \sin^2(\phi) + B_2 \cos^2(\phi) \quad (4)$$

It shows AVAZ response can be described as an elliptic equation. With opening angle gathers, extracting amplitudes along all azimuth, fracture strength  $B_2/B_1$  and its strongest direction  $\phi_{sym}$  are achieved.

We use reflection angle gathers for fracture inversion. In HTI media with vertical fractures, velocity variation with different azimuth is evident, and it will cause residual moveout. These residual moveout (RMO) on reflection angle gather looks like a saddle, so called snail gather, and it has to be corrected before extracting amplitudes for

AVAZ inversion. So a full flow of fracture prediction is proposed in Figure 8.

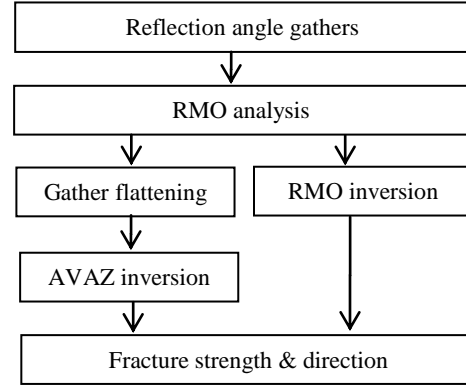


Figure 8: Fracture Prediction Workflow

The left branch is AVAZ inversion workflow. Residual moveout depending on azimuth velocity variation caused by fractures needs to be eliminated to flatten gathers, after that, the result of AVAZ inversion is reasonable. In the right branch, RMO inversion is used to derive azimuthal velocity variation and then fracture strength and orientation estimation. Because of the overburden's influence to velocity, the RMO inversion is not as reliable as AVAZ amplitude inversion.

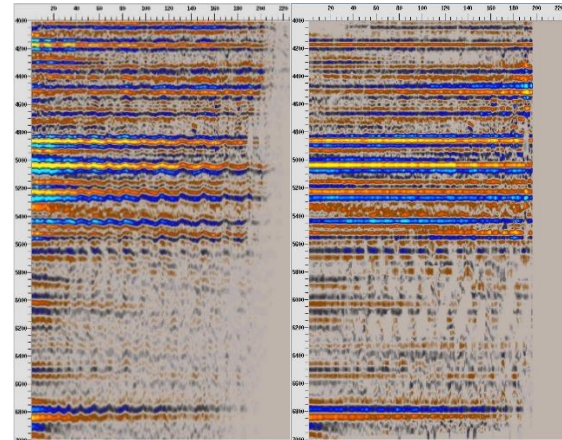


Figure 9: Reflection gather before(left) and after(right) geometrical spreading + Q-absorption, amplitude equalization + mute angles, continuity mute, automatic flattening

In figure 9 the reflection on the left shows obvious azimuthal variation. After a series of amplitude preserving processing techniques such as geometrical spreading, Q-absorption, amplitude equalization, continuity mute, the gather is flattened. After that, an AVAZ inversion is conducted to derive fracture strength and direction. Figure

## Local angle domain imaging and fracture prediction in Tarim Basin

10 shows fracture strength by color and fracture direction by vector sticks.

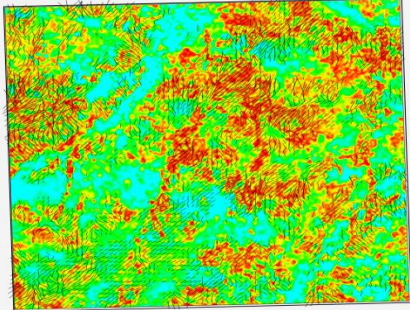


Figure 10: Fracture strength and direction in YM Area

In this survey, there are 8 wells with FMI imaging logging data acquired. Comparing AVAZ result inversion with FMI data, most of them are consistent. Therefore with a precise delineation of fracture in hand, we can plan wells with more confidence.

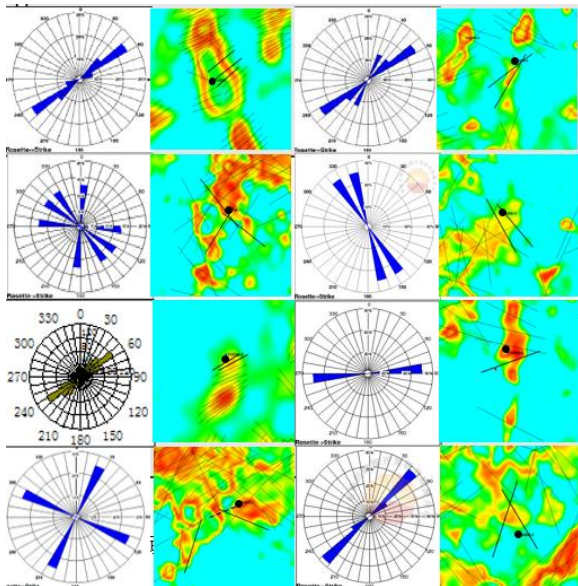


Figure 11. Imaging Logging vs AVAZ Inversion

### Conclusions

This paper introduced the method of local angle domain imaging, and analyzed two types of output gather and their features. These features are applicable for reservoirs in carbonate. In the examples, diffraction and specular reflection can be separated in dip angle domain, Karst carve images are enhanced and identification is improved. opening angle gathers provide two ways to invert fractures, which are residual moveout and amplitude depending on azimuth. Imaging logging confirms the accuracy of AVAZ.

In conclusion, local angle domain imaging is a low-cost method based on ray theory, the applications are various and flexible, and based on local angle domain imaging, the research on carbonate reservoirs in YM area have made great achievements.

### Acknowledgements

We thank Tarim Oilfield Company, PetroChina for the authorization to present this work.

### REFERENCES

Duan W. S., and F. Li, 2013, Analysis of multiple attenuation through pre-stack migration in OVT domain: 75th Conference & Exhibition, EAGE, Extended Abstracts, Th-P08-15, doi:10.3997/2214-4609.20130285.

Full-azimuth subsurface angle domain wavefield decomposition and imaging, GEOPHYSICS, VOL. 76, NO.1 JANUARY-FEBRUARY2011; P. S1-S13, 19 FIGS.10.1190/1.3511352

Anat Canning and Alex Malkin, Paradigm, Azimuthal AVA Analysis Using Full-Azimuth 3D Angle Gathers, SEG, Houston, 2009, International Exposition and Annual Meeting

Zvi Koren, EarthStudy 360 Specularity and Diffraction Operations, Houston, 2016